Naval Research Laboratory
Washington, DC 20375-5320

NRL/6120/MR—2023/4

Preparation of Cyclic PolyAcrylates for Improved Strength and Durability

MATTHEW D. THUM

Applied Concepts in Materials Branch
Chemistry Division

August 30, 2023

REPORT DOCUMENTATION PAGE

Form Approved
OMB No. 0704-0188

1. REPORT DATE *(DD-MM-YYYY)*	**2. REPORT TYPE**	**3. DATES COVERED** *(From - To)*
30-08-2023	NRL Memorandum Report	Feb 2022 – Feb 2023

4. TITLE AND SUBTITLE

Preparation of Cyclic PolyAcrylates for Improved Strength and Durability

5a. CONTRACT NUMBER

5b. GRANT NUMBER

5c. PROGRAM ELEMENT NUMBER

6. AUTHOR(S)

Matthew D. Thum

5d. PROJECT NUMBER

5e. TASK NUMBER

5f. WORK UNIT NUMBER
N21E

7. PERFORMING ORGANIZATION NAME(S) AND ADDRESS(ES)

Naval Research Laboratory
4555 Overlook Avenue, SW
Washington, DC 20375-5320

8. PERFORMING ORGANIZATION REPORT NUMBER

NRL/6120/MR--2023/4

9. SPONSORING / MONITORING AGENCY NAME(S) AND ADDRESS(ES)

Naval Research Laboratory
4555 Overlook Avenue, SW
Washington, DC 20375-5320

10. SPONSOR / MONITOR'S ACRONYM(S)
NRL

11. SPONSOR / MONITOR'S REPORT NUMBER(S)

12. DISTRIBUTION / AVAILABILITY STATEMENT

DISTRIBUTION STATEMENT A: Approved for public release; distribution is unlimited.

13. SUPPLEMENTARY NOTES

14. ABSTRACT

In this work a new class of cyclic chain transfer agents based on current RAFT agents and TARO-based RAFT agents are synthesized to prepare cyclic polymers using photoRAFT or PET-RAFT. Cyclic CTAs synthesized in this work were evaluated with a series of different monomers, and under various conditions, but no significant polymer formation was observed under any set of experimental conditions. Computational analysis determined that the geometry of the cyclic CTAs prepared in this study are not idea for C-S bond homolysis, and therefore are not expected to act as an iniferter in a photoRAFT process.

15. SUBJECT TERMS

Polymers Cyclic Polymers RAFT
photoRAFT Photochemistry

16. SECURITY CLASSIFICATION OF:			**17. LIMITATION OF ABSTRACT**	**18. NUMBER OF PAGES**	**19a. NAME OF RESPONSIBLE PERSON**
					Matthew D. Thum
a. REPORT	**b. ABSTRACT**	**c. THIS PAGE**	U	39	**19b. TELEPHONE NUMBER** *(include area code)*
U	U	U			(202) 404-1200

This page intentionally left blank.

1. Introduction.

Polymer properties are directly linked to their nanoscale architecture. Polymer chemists have strived to achieve more and better control over polymer architecture with the synthesis of linear, block, bottlebrush, star, dendrimeric, and hyperbranched polymers. Detailed studies of these and other polymeric networks has resulted in an understanding of the effects of covalent architecture on the macroscopic polymer properties. To this end, polymers with "continuous" cyclic topology have been the subject of recent and renewed interest because, in linear polymers, the presence of end groups has a significant impact on the material properties.[1-3] Despite the interest and potential applications, however, detailed analysis of cyclic polymers has been severely limited by synthetic complications and issues with linear impurities. Currently, there is a focus on preparing cyclic polymers for academic and industrial applications, but there still exist many challenges that need to be overcome to fully realize commercial success: the first is an efficient method of achieving high-purity samples, and secondly, is developing these methods for large-batch production. The proposed work aims to overcome these two challenges by: (1) developing a synthetic method using facile synthesis and commercially available starting materials which produces solely cyclic polymer product eliminating the need for complicated purifications steps, and (2) achieving cyclic topology by modifying a popular polymerization method, RAFT, which is already able to prepare polymers at scale enabling easy transition to commercial and Naval applications.

1.1 Physical Properties of Cyclic Polymers.

One of the main driving forces behind the development of new synthetic approaches towards preparing cyclic polymers is their unique physical properties. The lack of chain ends substantially affects the chain-chain interactions and causes cyclic polymers to deviate significantly from traditional behavior. Although there are many interesting physical properties of cyclic polymers, this brief introduction will focus on three that directly relate to their industrial applications; (1) glass transition temperature (T_g), (2) melt viscosity, and (3) thermostability.

Manuscript approved August 14, 2023.

The glass transition (T_g) of a polymer marks the reversible transition from a hard, brittle, material into a more-viscous rubbery state. Hard plastics are used at temperatures well below their T_g and rubbery materials as used at temperatures well above their T_g. Therefore, the T_g determines the upper working limit of a hard plastic before it becomes structurally unstable. Generally, T_g increases with increasing molecular weight asymptotically towards a value that would represent infinite chain length. Cyclic polymers have previously shown to have a higher T_g than their linear analogues, and possibly more importantly, the T_g of cyclic polymers has been found to be independent of the molecular weight. A study by Xu and coworkers showed a 30% increase in the T_g for a cyclic main-chain azobenzene polymer when as compared to the linear polymer.[4] For hard plastics such as polymethyl methacrylate (PMMA), which has a T_g of 105 °C, an increase in the T_g would represent an increase in the working environment and may extend its possible applications.

From an industrial standpoint, an important property of a polymer is its ease of processability. Melt viscosity is an important material property that measures the rate at which a material can be extruded through an orifice at a certain temperature and load. The melt viscosity directly relates to the ability of the polymer to be used in injection molding systems necessary for large-scale applications. The higher the viscosity of the polymer, the more difficult it becomes to process. Importantly, due to their unique cyclic topology, cyclic polymers have shown to have significantly lower melt viscosities than their linear analogues. Indeed, for polybutadiene, it was shown that polymers with cyclic topology had a 10 fold decrease in their melt viscosities when compared with linear polymers.[5]

The thermostability of a compound is the temperature at which the material breaks down irreversibly. A measure of the ability of the material to resist heat and maintain strength, elasticity, and toughness at elevated temperatures, the thermostabiltiy is important for determining the maximum temperature at which the polymer can be used. For cyclic polymers, increased packing due to the reduction of the polymer footprint leads to stronger, denser polymers with improved thermal properties. Specifically,

studies on macrocyclic poly(2-vinylnaphthalene) (P2VN) and poly(2-vinyl-9,9-dimethylfluorene) (PDMVF) showed improved thermostability over their linear analogues.[6]

1.2 Current Methods of Achieving Cyclic Polymers.

There are three main approaches for the preparation of cyclic polymers: (1) bimolecular ring closure, (2) unimolecular ring closure (homodifunctional and heterodifunctional), and (3) ring-expansion polymerization. A general schematic illustration of these methods is shown in figure 1.

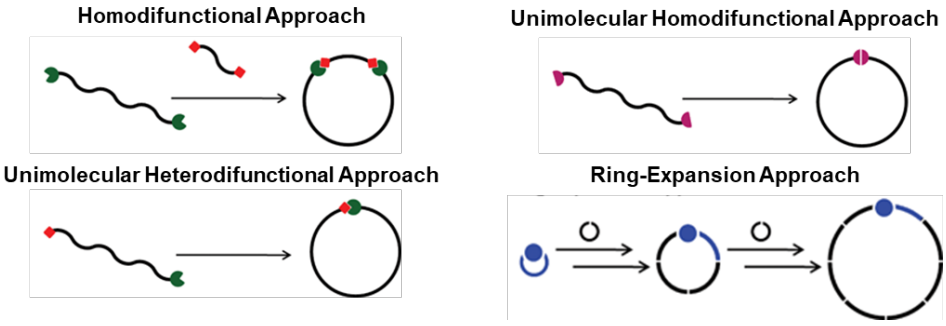

Figure 1. Schematic representation of common techniques for preparing cyclic polymers. Adapted from the following reference.[1]

Modern methods of preparing cyclic polymers are fairly robust and have demonstrated the ability to prepare well-defined cyclic polymers, but each has significant drawbacks. In both bimolecular and unimolecular ring closure reactions, there is competition between forming cyclic and linear polymers. This leads to significant linear impurities and can only be addresses by operating under highly dilute conditions, or with specifically designed monomers requiring complex synthesis. These constraints significantly limit the substrate scope of these ring closure reactions and the synthetic conditions drastically limit industrial applications. Ring-expansion polymerization, on the other hand, is an elegant alternative that involves the repeated insertion of a cyclic monomer into a cyclic catalyst/initiator. This avoids some of the drawbacks associated with ring closure reactions but requires very specific choice of monomer and results in very limited polymer backbone diversity, and thus, limits possible applications. The proposed work will aim to significantly broaden the substrate scope of cyclic polymers by developing new synthetic pathways using

photoinduced reversible addition fragmentation chain transfer (photoRAFT) polymerization. If successful, this work will enable the preparation of robust, functional materials that demonstrate the improved physical properties of current cyclic polymers while doing so using a facile and easily scalable synthetic method.

1.3 PhotoRAFT – Our Approach.

The proposed work will involve the development of a new method of preparing cyclic polymers based on photochemically activated reversible addition fragmentation chain transfer (photoRAFT) polymerization. By precisely controlling the photolysis of a cyclic chain transfer agent (CTA), cyclic polymers will be synthesized in high yield, and with minimal linear impurities.

Traditional RAFT is a multi-component system that requires a dithio-, or trithio-based chain transfer agent (CTA), monomer, and initiating species. The polymerization process is controlled by reversible deactivation of growing chains by the CTA allowing for propagation at the same rate across growing chains resulting in a final polymer with uniform distribution of polymer chain lengths and molecular weights. As a versatile method of controlled radical polymerization, photoRAFT has been the subject of recent and renewed interest. As opposed to traditional, thermally initiated, methods, photoRAFT uses light to control the rate of initiation allow for precise spatial and temporal control over the reaction process. Although there are several ways photoRAFT can be affected, this work will focus on the photoiniferter method in which the CTA serves as capping agent and initiator (figure 2).

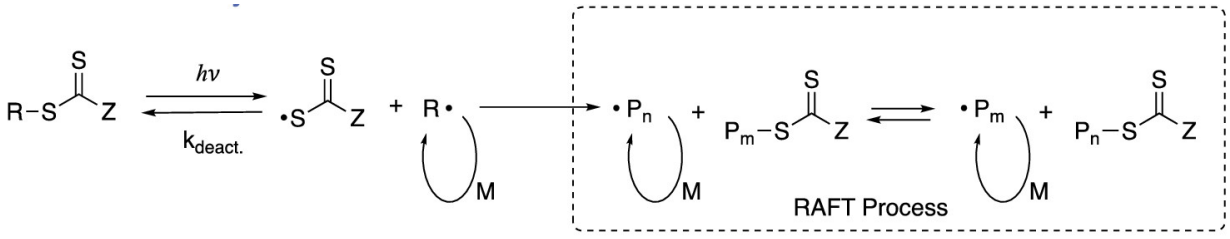

Figure 2. PhotoRAFT using the photoiniferter process. A CTA is irradiated generating a reactive, propagating, radical and a non-propagating, sulfur-centered radical.

First described by Otsu and coworkers, the photoiniferter method relies on photoinitiated C-S bond dissociation to generate the initiating/propagating and capping radical species.[7] The photoiniferter method has been employed with dithio- and trithio-based RAFT agents and has been activated with UV and visible light irradiation.[8-12] Building on the framework laid out by Otsu and others, herein we propose a new method of preparing cyclic polymers by employing photoRAFT on a cyclic CTA (figure 3).

Broadly, preparation of cyclic polymers using RAFT has been unsuccessful. Using photoRAFT will enable the preparation of cyclic polymers with a diverse range of possible monomers, significantly broadening the architectures that can be attained. This will be performed by the photolysis of a novel cyclic RAFT agent in the presence of acrylate monomers. Unlike traditional RAFT polymerization, using a direct photolysis initiation mechanism on a cyclic RAFT agent will result in propagation and chain growth by ring-expansion polymerization, and will result in majority cyclic product.

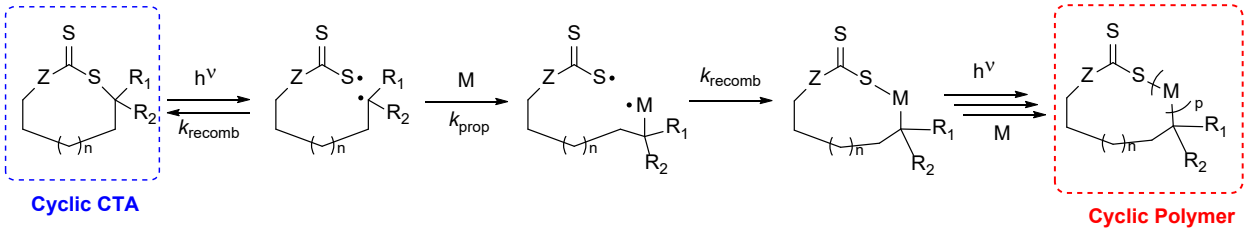

Figure 3. The preparation of a cyclic polymer using photoRAFT and a cyclic CTA. Photolysis of the cyclic CTA leads to homolytic C-S bond dissociation at the most substituted position. The resulting diradical is capable of recombination in the solvent cage to reform the starting material, however, in the presence of suitable concentration of monomer (M), the carbon-centered radical can add to the monomer in a classical free-radical propagation step. After monomer addition and radical recombination, a cyclic polymer is formed.

Preparing cyclic polymers in this way requires precise control over the photolysis of the CTA. This was not possible until a recent study by the Falvey group thoroughly described the photophysics of dithio- and trithio-based CTAs.[13] In the study, Falvey and coworkers measured the C-S bond dissociation of

common CTAs as a function of wavelength of irradiation, and degree of functionalization. Their work was vital to the proposed research because it demonstrated that the strength of the C-S bond can be synthetically tailored. It is important that the desired C-S bond dissociation is the sole result of photolysis to minimize formation of linear impurities. Another important conclusion from Falvey and coworkers is the observation of a free radical cage effect during photoRAFT using the iniferter method. Recombination of radicals within the solvent cage is paramount to achieving cyclic topology and avoiding crossover reactions. The results by Falvey and coworkers suggest that, in the absence of a high concentration of monomer, radical recombination is preferred ensuring that, in our system, there is little crossover between polymer chains. An example of some of their results showing the bond dissociation energy of a CTA with respect to the degree of functionalization is given in figure 4.

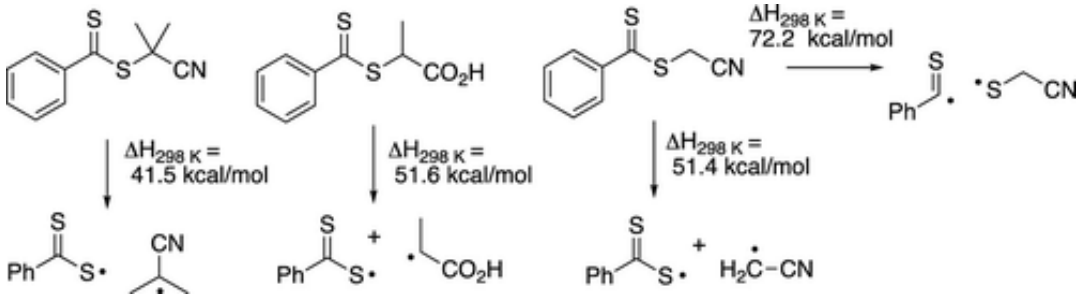

Figure 4. Comparison of calculated bond dissociation enthalpies for various dithioesters. Adapted from the following reference.[13]

The objective of this work is to synthesize a new class of acrylate polymers with cyclic topology and demonstrate improved mechanical properties when compared with linear polyacrylates. Specifically, the preparation of polyacrylates with cyclic topology will result in the ability to make less-dense, thinner, polymers with improved strength, durability, and ease of processing when compared with structurally similar linear polyacrylates. Success in this project will result in improvements upon current polyacrylates for use in Naval applications, such as windows in underwater submersibles, abrasion resistant covers for sensors, and heat resistant seals.

2. The Synthesis of Cyclic CTAs

A library of cyclic CTAs were synthesized and screened for efficiency in cyclic polymer production. Cyclic polymers are prepared by photoRAFT polymerization. If successful, this work will represent the sole example of the production of cyclic polymers using photoRAFT, and will be the only example of cyclic polymers generated by free radical polymerization without the use of a highly specific metal-center catalyst.

2.1 The Synthesis of Biphenyl-based (Thioacetyl Ring Opening, TARO) Cyclic RAFT Agents

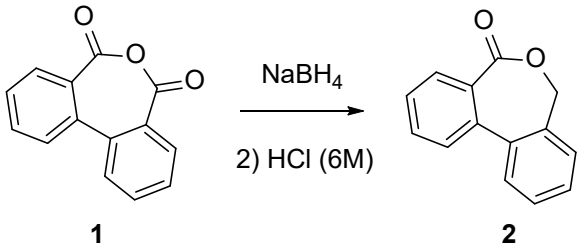

Figure 5. The synthesis of **2**.

The synthesis was adapted from the following procedure.[14] To a 100 mL round bottom flask, 8.0401 g (35.8 mmol) of **1** was added along with 50 mL DMF. The solution was cooled to 0 °C using an ice bath before 1.41 g $NaBH_4$ was added slowly. The solution becomes a clear yellow. The ice bath was removed, and the solution is allowed to stir at room temperature for 2 hours before it is slowly poured into a 250 mL Erlenmeyer flask containing 40 mL of 6M HCl. The mixture was stirred overnight and allowed to precipitate. The white solids were collected using vacuum filtration and dissolved in 100 mL DCM. The organic layer was washed with 2 x 100 mL water and 1 x 100 mL $NaHCO_3$. The organic layer was dried over $MgSO_4$ and the solvent was removed under vacuum yielding 5.79 g of **2** in 77% yield and this product was used subsequently without further purification. ^{1}H NMR (400 MHz, (CD_3Cl)) δ, ppm: 7.65 (d, 1H), 7.62-7.41 (m, 7H), 5.05 (d, 2H).

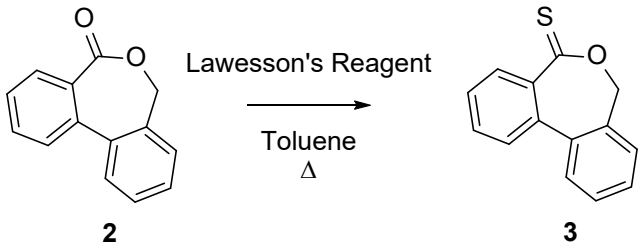

Figure 5. The synthesis of cyclic CTA, **3**.

The synthesis was adapted from the following procedure.[14] To a 500 mL round bottom flask was added 4.6917 g (22.29 mmol) **2** and 350 mL toluene. To this 5.3214 g (0.6 eq) of Lawesson's reagent was added and the solution was heated to reflux overnight. The mixture was concentrated *in vacuo* and purified by column chromatography (Hex-EtOAc, 4:1) to afford yellow crystals (2.07 g, 41% yield). ^{1}H NMR (400 MHz, (CD_3Cl)) δ, ppm: 7.68 (d, 1H), 7.66-7.41 (m, 7H), 5.06 (d, 2H).

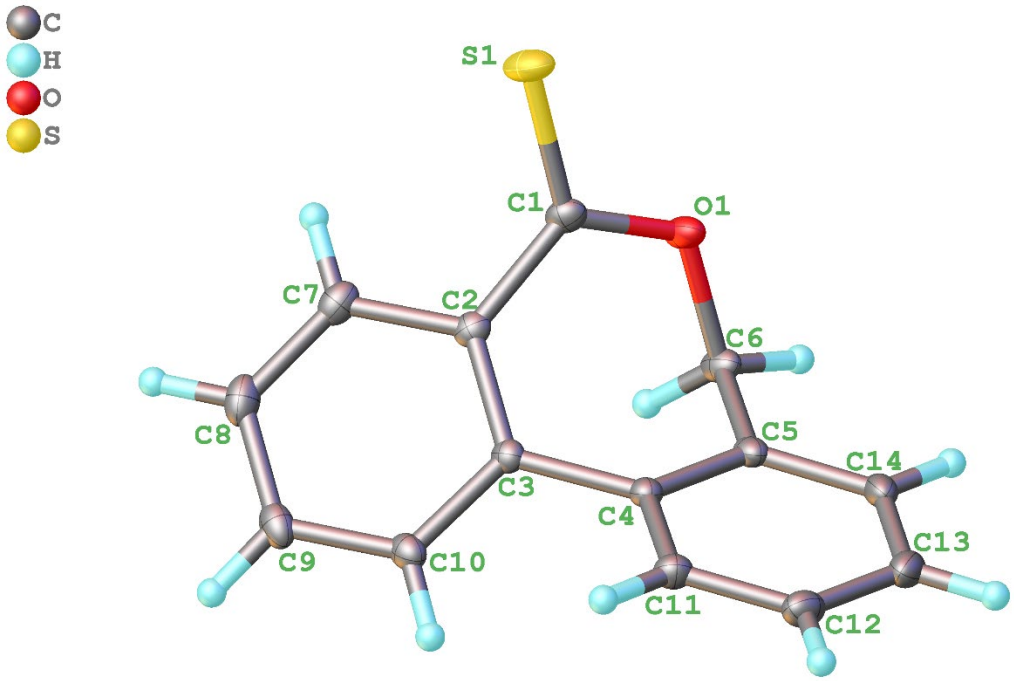

Figure 6. Single crystal structure of **3**.

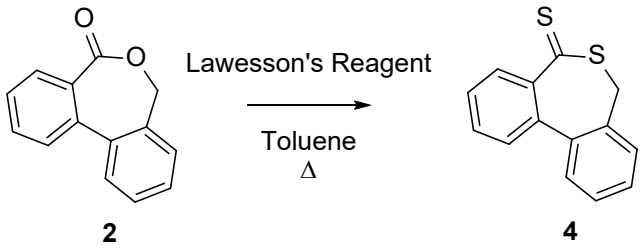

Figure 7. The synthesis of cyclic CTA, **4**.

The synthesis was adapted from the following procedure.[14] To a 500 mL round bottom flask was added 1.8085 g (8.6 mmol) **2** and 350 mL toluene. To this 7.6523 g (2.2 eq) of Lawesson's reagent was added and the solution was heated to reflux overnight. The mixture was concentrated *in vacuo* and purified by column chromatography (Hex-EtOAc, 4:1) to afford a red oil which crystalized on standing (225.7 mg, 10.8% yield). The majority of the product formed was **3.** ^{1}H NMR (400 MHz, (CD_3Cl)) δ, ppm: 7.56 (d, 1H), 7.54 (t, 1H), 7.45-7.32 (m, 5H), 7.28 (d, 1H), 4.44 (d, 1H), 3.53 (d, 1H).

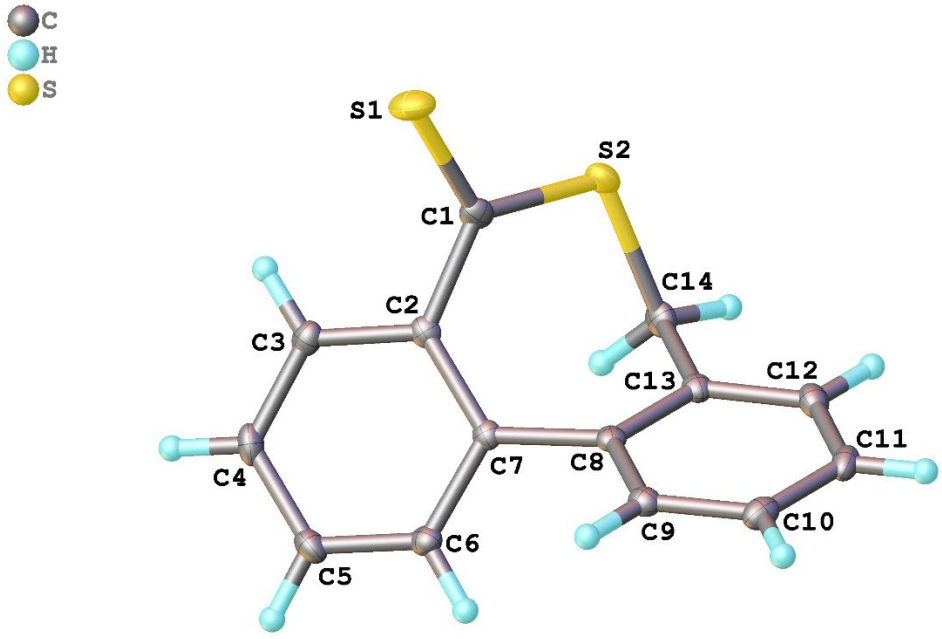

Figure 8. Single crystal structure of **4**.

2.2 The Synthesis of Cyclic Trithiocarbonate-based RAFT Agents using a Phase Transfer Catalyst

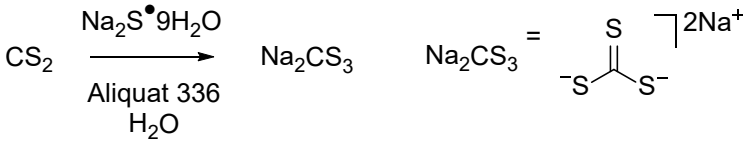

Figure 9. The synthesis of Na_2CS_3.

The synthesis was adapted from the following procedure.[15] To a 100 mL RBF was added 19.93 g $Na_2S•9H_2O$ (83 mmol), 6.6 g CS_2 (87 mmol) and 823 uL Aliquat 336 (1.8 mmol) in 30 mL H_2O. The solution was stirred at room temperature overnight. The solution became deep red resulting in a solution measuring 23 wt% Na_2CS_3 in water. The solution was used without further purification. The mixture was stored at 0 °C.

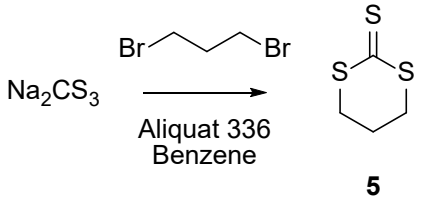

Figure 10. The synthesis of **5** from Na_2CS_3.

The synthesis was adapted from the following procedure.[16] In a 25 mL round bottom flask, 4 g of Na_2CS_3 (23 wt% in H_2O, 6 mmol) was added to 5 mL benzene. To this, 430 mg of 1,3-dibromobutane (240 µL, 2 mmol) and 40 µL Aliquat 336 (0.08 mmol) was added. The solution was heated to reflux overnight. The solution became yellow. After refluxing the reaction mixture overnight, it was poured into 20 mL of water and extracted with 2 x 20 mL EtOAc. The organic layers were collected and washed with 1 x 10 mL 10% HCl followed by 2 x 10 mL water. The organic layer was dried over $MgSO_4$ and removed *in vacuo*. Only trace amounts of **5** were detected using ^{1}HNMR. The mixture was unable to be adequately purified to be further used.

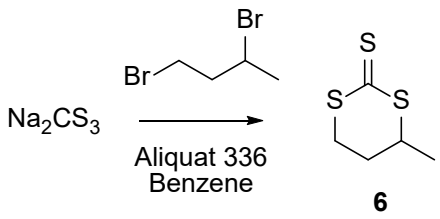

Figure 11. The synthesis of **6** from Na_2CS_3.

The synthesis was adapted from the following procedure.[16] In a 25 mL round bottom flask, 4g of Na_2CS_3 (24 wt% in H_2O, 6 mmol) was added to 5 mL benzene. To this, 404 mg of 1,3-dibromobutane (203 µL, 2 mmol) and 40 µL Aliquat 336 (0.08 mmol) was added. The solution was heated to reflux overnight. The solution became yellow. After refluxing the reaction mixture overnight, it was poured into 20 mL of water and extracted with 2 x 20 mL EtOAc. The organic layers were collected and washed with 1 x 10 mL 10% HCl followed by 2 x 10 mL water. The organic layer was dried over $MgSO_4$ and removed *in vacuo*. Only trace amounts of **6** were detected using ^{1}HNMR. The mixture was unable to be adequately purified to be further used.

2.3 The Synthesis of Cyclic Trithiocarbonate-based RAFT Agents using Cs_2CO_2/CS_2

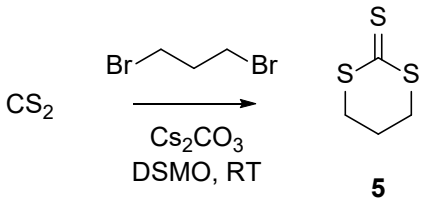

Figure 12. The synthesis of **5** from CS_2.

The synthesis was adapted from the following procedure.[17] Carbon disulfide (CS_2, 761 mg, 10 mmol) and 10 mL DMSO were added to a 10 dr. vial. To this, 3.26 g Cs_2CO_3 was added and the solution turned deep red. While stirring, 1,3 dibromopropane (2.019 g, 10 mmol) was added dropwise and the mixture became chalky yellow. The vial was sealed and stirred at 30 °C overnight using a block heater before being poured into 50 mL DI water. The product was extracted with ethyl acetate 2 x 50 mL and the combined organic layers were dried using anhydrous Na_2SO_4 and concentrated *in vacuo*. The resulting

yellow oil was purified using column chromatography (10:1 Hexanes/EtOAc) to yield 1.1 g of **5** as a yellow crystalline solid in 73% yield. ^{1}H NMR (400 MHz, (CD_3Cl)) δ, ppm: 3.22 (t, 1H), 2.42 (m, 2H). The crystals were of suitable quality to obtain a crystal structure given in figure 13.

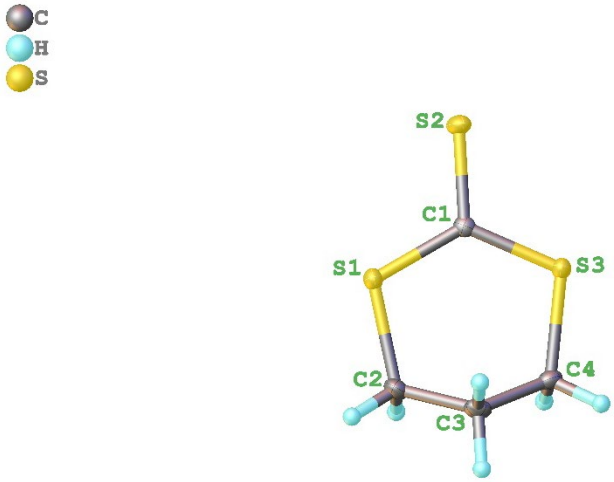

Figure 13. Single crystal structure of **5**.

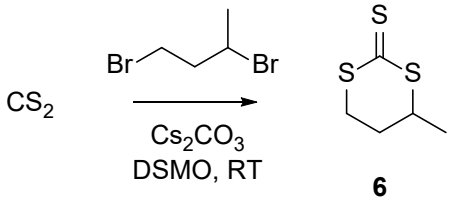

Figure 14. The synthesis of **6** from CS_2.

The synthesis was adapted from the following procedure.[17] Carbon disulfide (CS_2, 761 mg, 10 mmol) and 10 mL DMSO were added to a 10 dr. vial. To this, 3.26 g Cs_2CO_3 was added and the solution turned deep red. While stirring, 1,3 dibromobutane (2.15 g, 10 mmol) was added dropwise and the mixture became chalky yellow. The vial was sealed and stirred at 30 °C overnight using a block heater before being poured into 50 mL DI water. The product was extracted with ethyl acetate 2 x 50 mL and the combined organic layers were dried using anhydrous Na_2SO_4 and concentrated *in vacuo*. The resulting yellow oil was purified using column chromatography (10:1 Hexanes/EtOAc) to yield 0.93 g of **6** as a yellow crystalline

solid in 60.5% yield. ^{1}H NMR (400 MHz, (CD_3Cl)) δ, ppm: 3.50 (m, 1H), 3.33-3.18 (m, 2H), 2.55 (m, 1H), 1.98 (m, 1H), 1.41 (d, 3H). The crystals were of suitable quality to obtain a crystal structure given in figure 15.

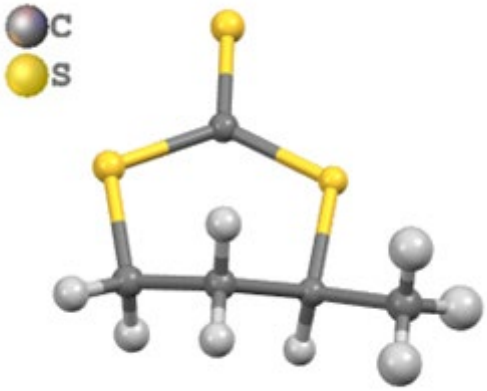

Figure 15. Single crystal structure of **6**.

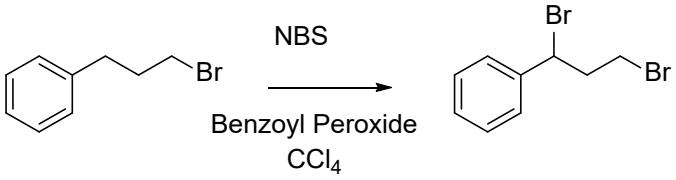

Figure 16. The synthesis of (1,3-dibromorpropyl)benzene.

The synthesis was adapted from the following procedure.[18] In a 25 ml RBF, N-bromosuccinimide (NBS, 0.9 g, 5.5 mmol) was added to solution of benzoyl peroxide (35 mg, 3 mol%) in 10 mL CCl_4. To this, 1-bromo-3-phenylpropane (1.01 g, 5 mmol) was added dropwise. After addition, the mixture was refluxed overnight before being cooled to room temperature and filtering through a pad of celite. The solvent was removed *in vacuo* resulting in (1,3-dibromorpropyl)benzene as clear oil which was used without further purification. ^{1}H NMR (400 MHz, (CD_3Cl)) δ, ppm: 7.41-7.31 (m, 5H), 5.19 (dd, 1H), 3.54 (m, 1H), 3.42 (m, 1H), 2.79 (m, 1H), 2.73 (m, 1H)

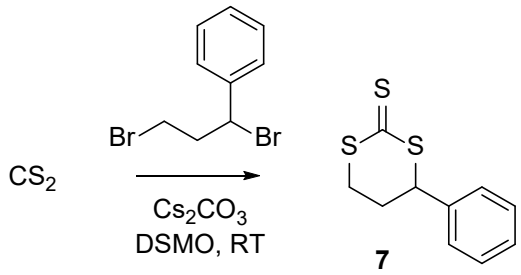

Figure 17. The synthesis of **7** from CS_2 and (1,3-dibromorpropyl)benzene.

The synthesis was adapted from the following procedure.[17] Carbon disulfide (CS_2, 0.92 mg, 12.1 mmol) and 12 mL DMSO were added to a 25 mL RBF. To this, 7.89 g Cs_2CO_3 (24 mmol) was added and the solution turned deep red. While stirring, (1,3-dibromorpropyl)benzene (3.36 g, 12.1 mmol) was added dropwise and the mixture became dark yellow. The RBF was stirred at RT overnight before being poured into 50 mL DI water. The product was extracted with ethyl acetate 2 x 50 mL and the combined organic layers were dried using anhydrous Na_2SO_4 and concentrated *in vacuo*. The resulting yellow oil was purified using column chromatography (10:1 Hexanes/EtOAc) to yield 1.63 g of **5** as a yellow solid in 60.3% yield. ^{1}H NMR (400 MHz, (CD_3Cl)) δ, ppm: 7.36 (m, 5H), 4.59 (dd, 1H), 3.40 (m, 1H), 3.24 (m, 1H), 2.80 (m, 1H), 2.52 (m, 1H)

3. Photophysical Properties of RAFT Agents

RAFT agents synthesized in this work were characterized using UV/Vis spectroscopy to determine the λ_{max} for the n→π* and π→π* transitions. Absorbance spectra were collected in methanol on an Agilent 8453 UV-Visible spectrophotometer 190 - 700 nm, and subsequently analyzed with Chemstation software. The absorbance spectra of the TARO-based RAFT agents, **3** and **4** are given in figures 18 and 19. The xanthate-like compound **3** is a yellow crystalline material which has a strong n→π* transition at 427 nm with a molar absorptivity (ε) of 350 M^{-1}•cm^{-1} and a broad π→π* transition at 310 nm with a ε of 7500 M^{-1}•cm^{-1}. The disulfide-based RAFT agent, on the other hand, is a red crystalline material with absorbance bands at 515 nm and 331 nm corresponding to the n→π* and π→π* transitions respectively.

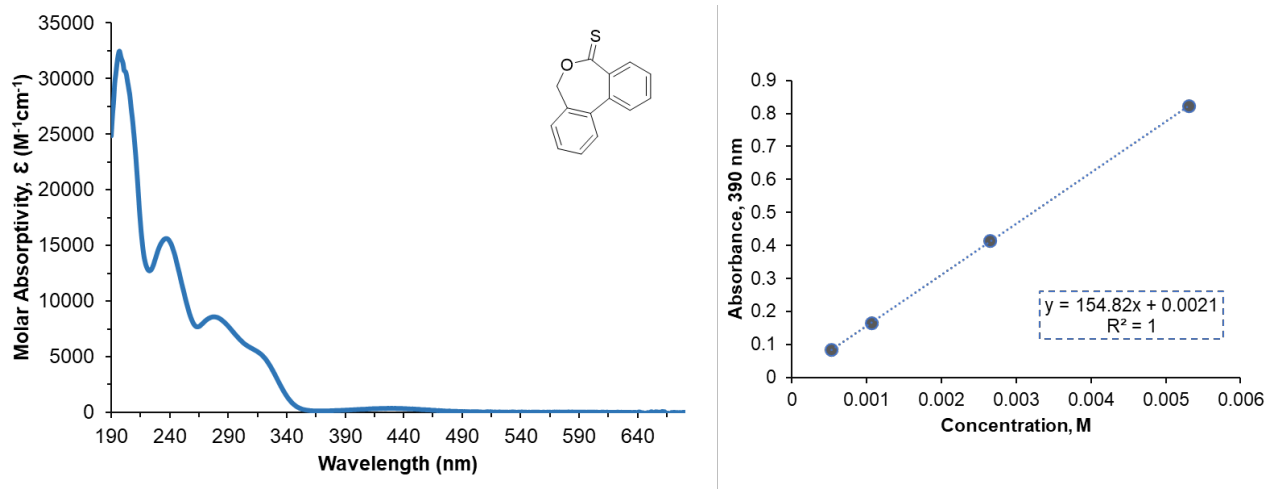

Figure 18. Absorbance spectra and ε calibration curve for **3** in methanol.

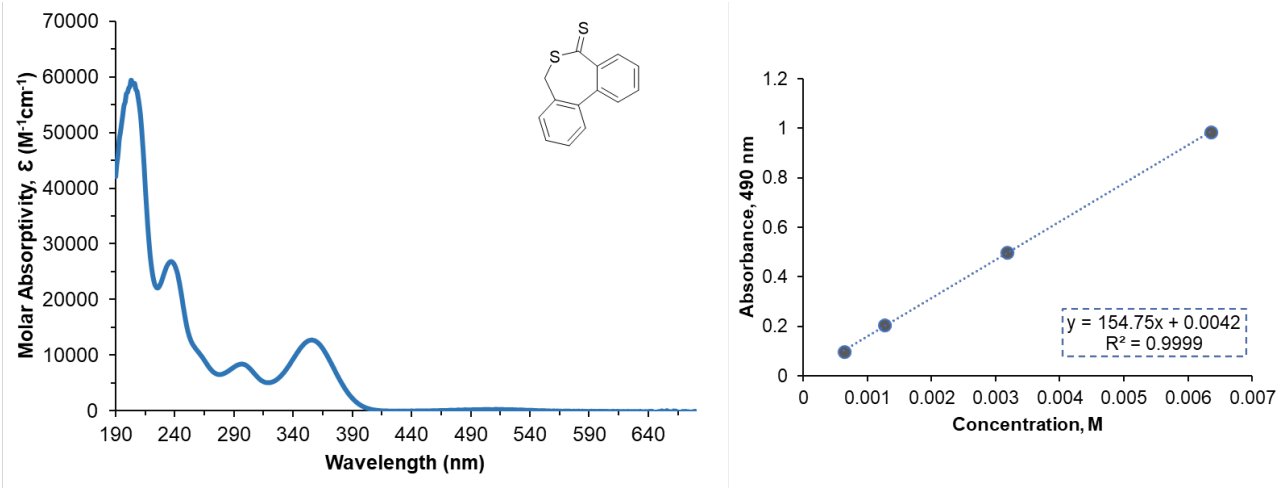

Figure 19. Absorbance spectra and ε calibration curve for **4** in methanol.

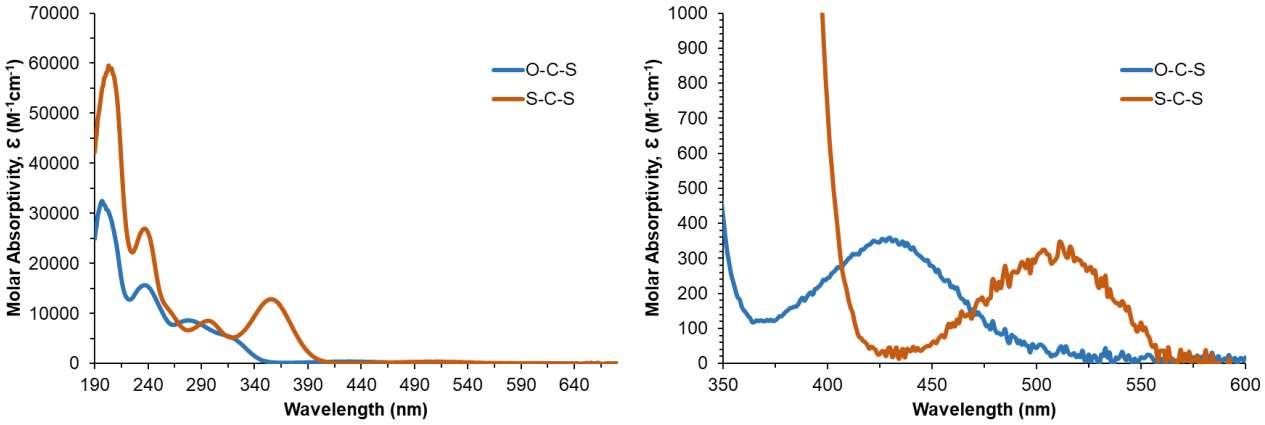

Figure 20. Absorbance spectra of **3** (blue) and **4** (orange) overlaid. *Right*: The difference in the n →π* transitions are highlighted.

Cyclic trithiocarbonates appear yellow and have transitions at ca. 450 nm and 350 nm. Both compounds **5** and **6** have similar, in intensity and wavelength, π→π* transitions at 340 nm, but the n→π* transition of **5** is noticeably stronger than **6** suggesting that orbital overlap is stronger for the unsubstituted ring. The phenyl-substituted RAFT agent, **7**, has similar transitions as **5** and **6**, although they are noticeably weaker. Indeed, the n→π* is extremely weak ($\varepsilon < 50\ M^{-1}\bullet cm^{-1}$ suggesting that the phenyl ring significantly suppresses the transition.

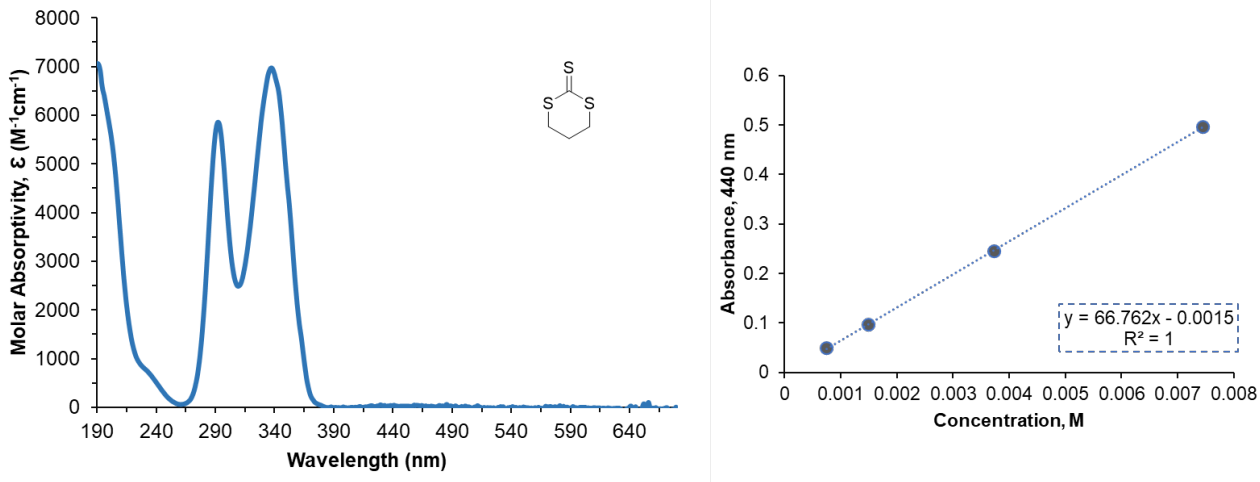

Figure 21. Absorbance spectra and ε calibration curve for **5** in methanol.

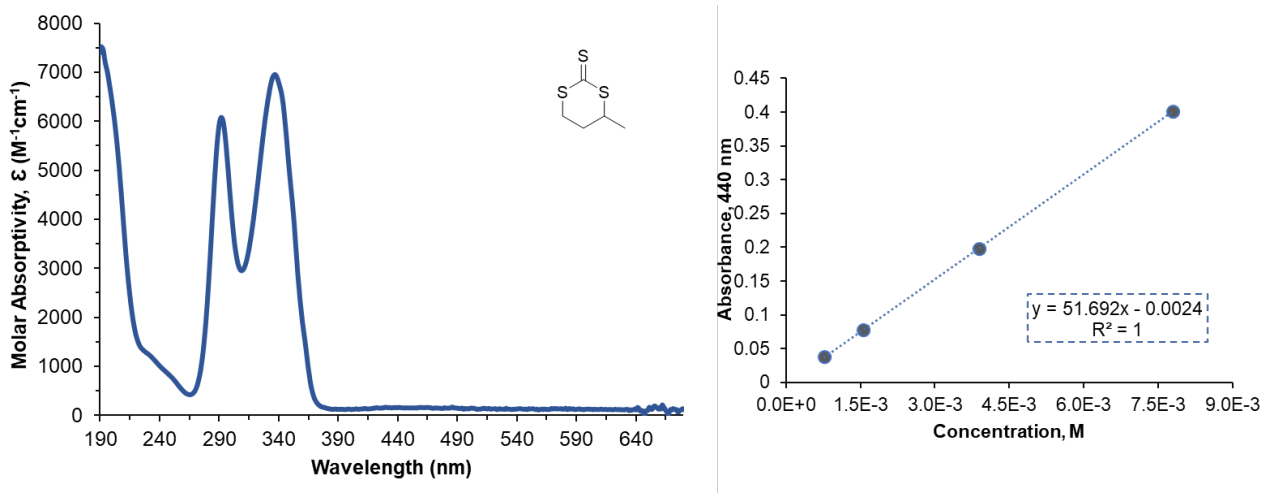

Figure 22. Absorbance spectra and ε calibration curve for **6** in methanol.

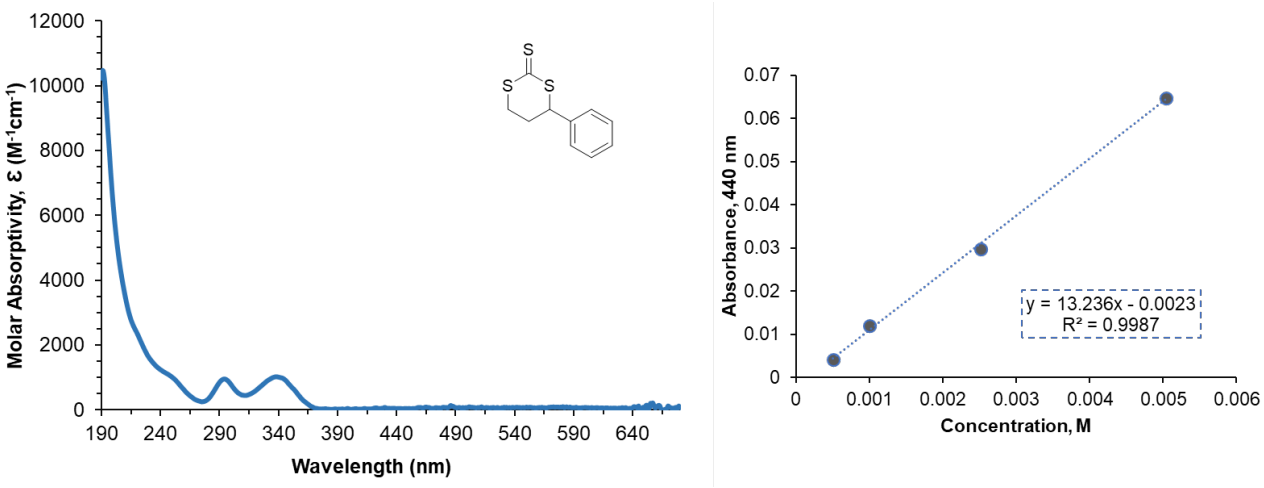

Figure 23. Absorbance spectra and ε calibration curve for **7** in methanol.

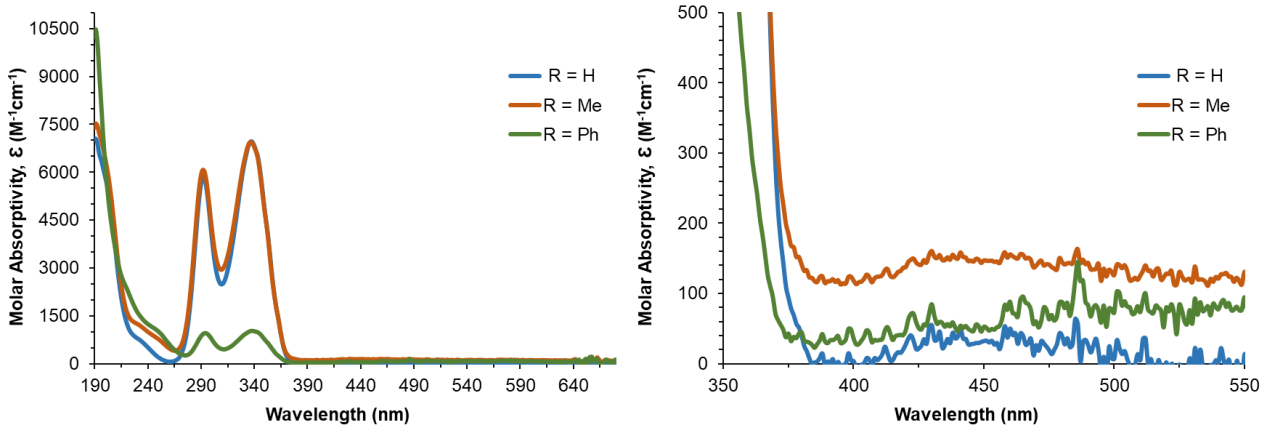

Figure 24. Absorbance spectra of **5**-**7** overlaid. *Right*: The difference in the n →π* transitions are highlighted.

4. Photopolymerization Using Cyclic RAFT Agents.

4.1 Generalized Polymerization Procedure.

In a 3.5 dr vial, monomer, solvent and CTA were added and the solution was sonicated in the absence of light until everything dissolved. The vial was sealed with a septum and purged with argon for 10 min in the solution and an additional 5 min in the headspace. Polymerizations were carried out under irradiation at different wavelengths using either a Rayonet photoreactor (365, or 300 nm), or a custom-built LED setup (395, 460, or 525 nm, Waveform Lighting). Unless otherwise noted, the conversion was measured by taking a small (≈10 μL) amount of the mixture and adding it to 0.5 mL of CD_3Cl for ^1H NMR. A typical polymerization is carried out either in 1 mL of neat monomer, or with 1 mL of DSMO and 1 mL of monomer. The theoretical molecular weights were calculated using eq. 1.

$$M_{n,th} = \frac{[M]_0 p M_M}{[CTA]_0} + M_{CTA} \qquad [1]$$

Where $[M]_0$ is the initial concentration of monomer, ρ is the polymerization efficiency, M_M is the molecular weight of the monomer, $[CTA]_0$ is the initial concentration of the CTA and M_{CTA} is the molecular weight of the CTA. The structures of the CTAs and monomers used in this work are given in figure 25.

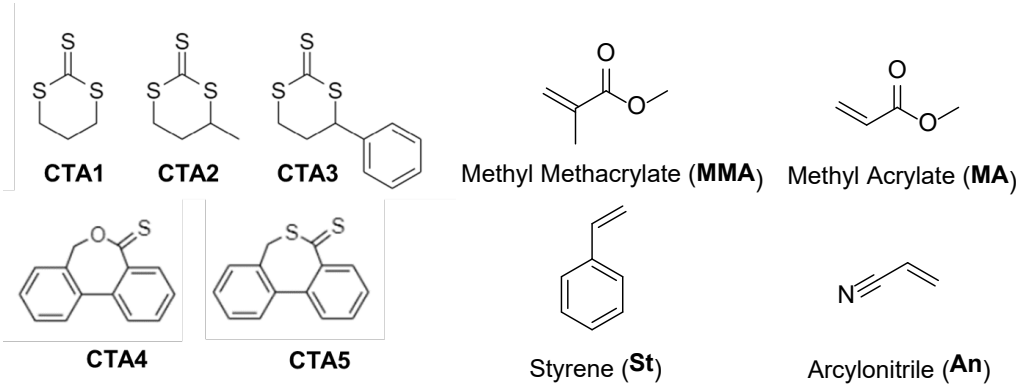

Figure 25. Compounds used in this study and abbreviations.

4.2 Photopolymerization Using Cyclic Trithiocarbonates.

Cyclic trithiocarbonates (CTA1-CTA3) were used as an iniferter in a photoRAFT process. As noted earlier in figures 21-24, cyclic trithiocarbonates have strong n→π* transitions at ca. 450 nm and a strong π→π* transition in the UV at ca. 340. Polymerizations were either carried out under broadband UV irradiation at 300 nm, or using LEDs at 395 or 460 nm as the irradiation source. Polymerizations were carried out for 18 hrs under argon with two different [M]/CTA ratios. A summary of the reactions performed can be found in Tables 1-4. For a given RAFT agent, the substituents determine the type of monomer that can be used.[19] Although the CTAs used in this work should be able to activate many different monomers, a variety of monomers with different activities from least active (An) to most active (St, MA, MMA) were chosen.

Many previous studies have shown that trithiocarbonates can be used as a photoiniferter in a RAFT process under UV irradiation.[20, 21] However, UV irradiation is known to cause unwanted degradation, low

conversion, loss of end group fidelity, and poor oxygen tolerance. Tables 1-3 shows the polymerization of CTA1-CTA3 using 300 nm light.

Table 1. Polymerization of cyclic trithiocarbonates at 300 nm

Monomer	[M]/CTA	Mw_{theo}	Conversion (CTA 1)	Conversion (CTA 2)	Conversion (CTA 3)
MMA	**-**	**-**	**N**	**N**	**N**
MA	**-**	**-**	**N**	**N**	**N**
An	**-**	**-**	**N**	**N**	**N**
St	**-**	**-**	**N**	**N**	**N**
MMA	**100/0**	**≈ 10k**	**N**	**N**	**Trace**
MMA	**200/0**	**≈ 20k**	**N**	**N**	**Trace**
MA	**100/0**	**≈ 10k**	**N**	**N**	**Trace**
MA	**200/0**	**≈ 20k**	**N**	**N**	**Trace**
An	**100/0**	**≈ 10k**	**N**	**N**	**Trace**
An	**200/0**	**≈ 20k**	**N**	**N**	**Trace**
St	**100/0**	**≈ 10k**	**N**	**N**	**Trace**
St	**200/0**	**≈ 20k**	**N**	**N**	**Trace**

*** in 1:1 by volume DMSO/Monomer **under argon**

Irradiation of CTA1-CTA3 at 300 nm in the presence of different monomers did not result in significant polymerization, or conversion. Due to the unstable radical that would result from C-S bond dissociation, CTA1 is not expected to efficiently initiate polymerization. However, CTA2 and CTA3 are

both expected to undergo C-S bond homolysis, but no polymer was detected by ^{1}H NMR regardless of the monomer employed.

Table 2. Polymerization of cyclic trithiocarbonates at 395 nm

Monomer	[M]/CTA	Mw_{theo}	Conversion (CTA 1)	Conversion (CTA 2)	Conversion (CTA 3)
MMA	**-**	**-**	**N**	**N**	**N**
MA	**-**	**-**	**N**	**N**	**N**
An	**-**	**-**	**N**	**N**	**N**
St	**-**	**-**	**N**	**N**	**N**
MMA	**100/0**	**≈ 10k**	**Trace**	**Trace**	**Trace**
MMA	**200/0**	**≈ 20k**	**Trace**	**Trace**	**Trace**
MA	**100/0**	**≈ 10k**	**Trace**	**Trace**	**Trace**
MA	**200/0**	**≈ 20k**	**Trace**	**Trace**	**Trace**
An	**100/0**	**≈ 10k**	**Trace**	**Trace**	**Trace**
An	**200/0**	**≈ 20k**	**Trace**	**Trace**	**Trace**
St	**100/0**	**≈ 10k**	**Trace**	**Trace**	**Trace**
St	**200/0**	**≈ 20k**	**Trace**	**Trace**	**Trace**

*** in 1:1 by volume DMSO/Monomer **under argon**

Likewise, irradiation of CTA1-CTA3 at 395 nm in the presence of different monomers did not result in significant polymerization, nor conversion. Although it is unsurprising that no polymer was seen for CTA1, the same lack of conversion was observed for CTAs 2 and 3 as well. Although it is possible that

395 nm irradiation was unsuccessful due to the lack of a strong absorbance band at that wavelength, it is unlikely. Recently, the Sumerlin group has investigated the effect of wavelength on the polymerization efficiency of photoRAFT agents and reported that irradiation of the n→π* band is the most efficient for photoRAFT agents.[22, 23] Based on these results, polymerizations using CTA1-CTA3 were carried out using 460 nm irradiation (Table 3).

Table 3. Polymerization of cyclic trithiocarbonates at 460 nm

Monomer	[M]/CTA	Mw_{theo}	Conversion (CTA 1)	Conversion (CTA 2)	Conversion (CTA 3)
MMA	**-**	**-**	**N**	**N**	**N**
MA	**-**	**-**	**N**	**N**	**N**
An	**-**	**-**	**N**	**N**	**N**
St	**-**	**-**	**N**	**N**	**N**
MMA	**100/0**	**≈ 10k**	**N**	**N**	**Trace**
MMA	**200/0**	**≈ 20k**	**N**	**N**	**Trace**
MA	**100/0**	**≈ 10k**	**N**	**N**	**Trace**
MA	**200/0**	**≈ 20k**	**N**	**N**	**Trace**
An	**100/0**	**≈ 10k**	**N**	**N**	**Trace**
An	**200/0**	**≈ 20k**	**N**	**N**	**Trace**
St	**100/0**	**≈ 10k**	**N**	**N**	**Trace**
St	**200/0**	**≈ 20k**	**N**	**N**	**Trace**

*** in 1:1 by volume DMSO/Monomer **under argon**

Despite previous studies indicating that visible light irradiation is the most likely to induce polymerization for CTA1-CTA3, only trace amounts of polymer were observed for CTA3 after overnight irradiation.[23] The lack of observed polymer regardless of monomer used suggests that C-S bond homolysis cannot be achieved through direct irradiation. However, previous work has shown that, despite DMSO being widely considered one of the best solvents for RAFT polymerization, the solvent can have a negative effect on polymerization efficiency, molecular weight control, and end group fidelity.[24] To examine the effects of solvent on the polymerization process, CTA3 was irradiated in neat monomer (Table 4). A representative ^{1}H NMR for following polymer conversion is given in figure 25.

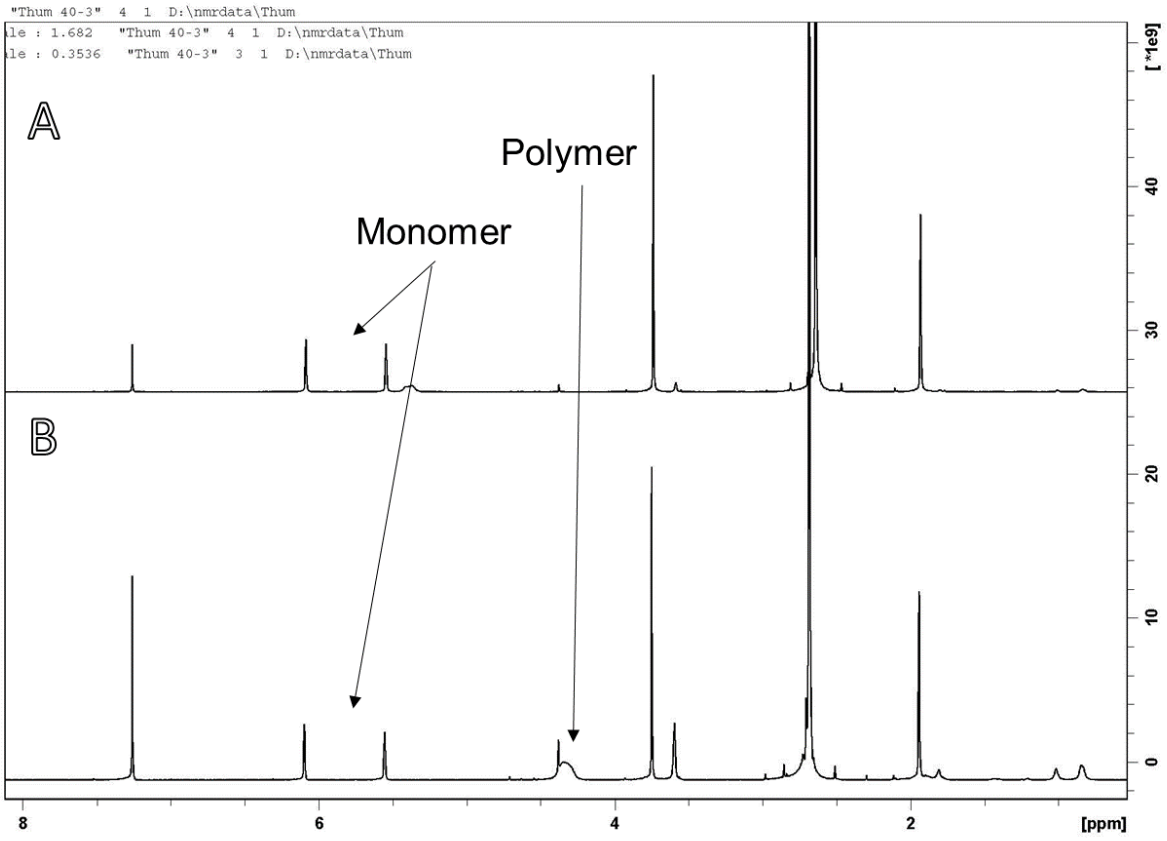

Figure 25. ^{1}H NMR of PET-RAFT polymerization of MMA with CTA2 in DMSO after 18 hrs of irradiation at (A) 460 nm and (B) 395 nm.

Table 4. Polymerization of CTA3 in neat monomer at 460 nm

Monomer	[M]/CTA	Mw_{theo}	Conversion (CTA 3)
MMA	**-**	**-**	**Trace**
MA	**-**	**-**	**Trace**
An	**-**	**-**	**Trace**
St	**-**	**-**	**Trace**
MMA	**100/0**	**≈ 10k**	**Trace**
MMA	**200/0**	**≈ 20k**	**Trace**
MA	**100/0**	**≈ 10k**	**Trace**
MA	**200/0**	**≈ 20k**	**Trace**
An	**100/0**	**≈ 10k**	**Trace**
An	**200/0**	**≈ 20k**	**Trace**
St	**100/0**	**≈ 10k**	**Trace**
St	**200/0**	**≈ 20k**	**Trace**

***under argon**

Only trace amounts of polymer were observed when performing the polymerization in the absence of solvent. This rules out low concentrations as a reason for the lack of polymer production. In all cases, the trace polymer obtained is most likely due to the effects of residual heating during the overnight irradiation and not as a result of direct CTA irradiation.

4.3 Photopolymerization Using Cyclic TARO Based RAFT Agents.

Thionolactone CTAs (CTA4 and CTA5) used in this work have been recently developed for degradable polymers by Gutenkunst, Johnson and others.[14, 25-27] Based on the initial CTA design by Meijs and Rizzardo, thionolactones are designed to ring-open to create polymers with main-chain thioesters that can be later cleaved to break down the polymer.[28] In this work, the ability of TARO-based CTAs to act as photoiniferters in a photoRAFT process was investigated.

The absorption spectra of the CTA4 and CTA5 are significantly different. As noted earlier in Figures 18-20, CTA4 has an n→π* transition at ca. 430 nm and a π→π* transition in the UV at ca. 300. CTA5, on the other hand, absorbs deeper to the red which is characteristic of dithioesters. It has an n→π* transition at ca. 530 nm and a π→π* transition in the UV at ca. 340. Polymerizations were carried out using LEDs at 395, 460 or 525 nm as the irradiation source. Polymerizations were carried out for 18 hrs under argon with two different [M]/CTA ratios. A summary of the reactions performed can be found in Tables 5-7.

Table 5. Polymerization of CTA4 at 460 nm

Monomer	[M]/CTA	Mw_{theo}	Conversion
MMA	**-**	**-**	**N**
MA	**-**	**-**	**N**
An	**-**	**-**	**N**
St	**-**	**-**	**N**
MMA	**100/0**	**≈ 10k**	**N**
MMA	**200/0**	**≈ 20k**	**N**
MA	**100/0**	**≈ 10k**	**N**

MA	**200/0**	**≈ 20k**	**N**
An	**100/0**	**≈ 10k**	**N**
An	**200/0**	**≈ 20k**	**N**
St	**100/0**	**≈ 10k**	**N**
St	**200/0**	**≈ 20k**	**N**

*** in 1:1 by volume DMSO/Monomer**
****under argon**

Table 6. Polymerization of CTA5 at 525 nm

Monomer	[M]/CTA	Mw_{theo}	Conversion
MMA	**-**	**-**	**N**
MA	**-**	**-**	**N**
An	**-**	**-**	**N**
St	**-**	**-**	**N**
MMA	**100/0**	**≈ 10k**	**N**
MMA	**200/0**	**≈ 20k**	**N**
MA	**100/0**	**≈ 10k**	**N**
MA	**200/0**	**≈ 20k**	**N**
An	**100/0**	**≈ 10k**	**N**
An	**200/0**	**≈ 20k**	**N**
St	**100/0**	**≈ 10k**	**N**

St	**200/0**	**≈ 20k**	**N**

*** in 1:1 by volume DMSO/Monomer**
****under argon**

Visible light irradiation of either CTA4 at 460 nm, or CTA5 at 525 nm, in the presence of monomer did not result in polymer formation. Neither changing the activity of the monomer nor changing the concentration of CTA had any effect on the reaction. The lack of polymer formation suggests that either the diradical resulting from C-S bond homolysis is too short-lived to react with a monomer, or more likely, homolysis from the excited state of the CTA is endergonic. The results from 395 nm irradiation of CTA4 and CTA5 can be found in Tables 4 and 5.

Table 7. Polymerization of TARO based CTAs at 395 nm

Monomer	[M]/CTA	Mw_{theo}	Conversion (CTA4)	Conversion (CTA5)
MMA	**-**	**-**	**N**	**N**
MA	**-**	**-**	**N**	**N**
An	**-**	**-**	**N**	**N**
St	**-**	**-**	**N**	**N**
MMA	**100/0**	**≈ 10k**	**Trace**	**Trace**
MMA	**200/0**	**≈ 20k**	**Trace**	**Trace**
MA	**100/0**	**≈ 10k**	**Trace**	**Trace**
MA	**200/0**	**≈ 20k**	**Trace**	**Trace**
An	**100/0**	**≈ 10k**	**Trace**	**Trace**
An	**200/0**	**≈ 20k**	**Trace**	**Trace**

St	**100/0**	**≈ 10k**	**Trace**	**Trace**
St	**200/0**	**≈ 20k**	**Trace**	**Trace**

*** in 1:1 by volume DMSO/Monomer **under argon**

Although there was trace polymer formation when irradiating CTA4 and CTA5 at 395 nm in the presence of monomer, the color of the solution was completely bleached after overnight photolysis suggesting CTA decomposition. Despite the decomposition of the CTA, no significant conversion was observed once again suggesting no significant radical formation. And due to the decomposition of CTA, 395 nm is a poor choice of wavelength for future experiments.

4.4. Photopolymerization by a PET-RAFT Process Using Cyclic RAFT Agents .

As an alternative approach to direct irradiation, Hawker, Boyer, Sumerlin and others employ photoredox catalysis to trigger the initiation step through reduction of the RAFT agent.[13, 19, 21] Photocatalysts are strong excited-state oxidants or reductants which can be used to activate the RAFT agent through and energy transfer or mediated electron transfer process. The photocatalytic PET approach is attractive as it generally results in less undesired degradation of the products due to the longer wavelengths of light employed during the polymerization process. A general scheme for the activation of a RAFT agent via. electron or energy transfer is given below in scheme 1.

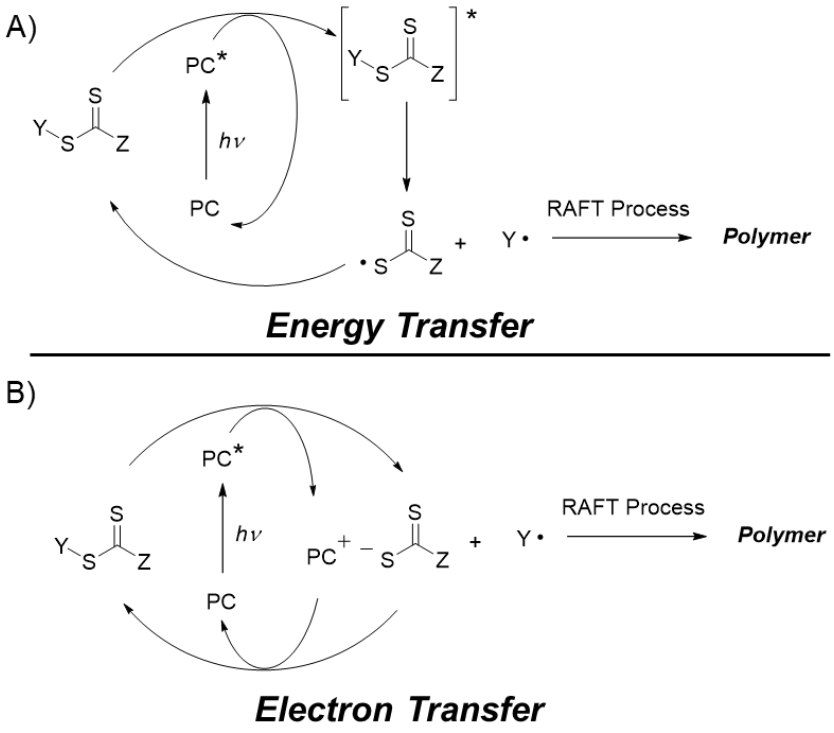

Scheme 1. The mechanism of PET-RAFT initiated by energy transfer (A) and electron transfer (B). The RAFT process is the same for both mechanisms.

PET-RAFT polymerization of cyclic trithiocarbonates can be found in table 8. Eosin Y was chosen as the photocatalysts because of its extensive use in PET-RAFT systems.[13, 21, 29, 30] Two separate systems were examined using Eosin Y as the photocatalyst. The first is an energy transfer system where no electro donor is added to the system and the second is a PET system using triethyl amine (TEA) as a sacrificial electron donor. Reactions were carried out in 1:1 DMSO/MA with irradiation at 525 nm which is near the λ_{max} of Eosin Y. For the cyclic trithiocarbonates, reactions were performed with either CTA2 or CTA3. No significant polymer formation was observed for any reaction conditions tested. A representative ^{1}H NMR showing the results of the polymerization reaction for CTA3 is given in Figure 26.

Table 8. PET-RAFT polymerization of Cyclic Trithiocarbonates

[M]/[CTA]/[EY]/[TEA]	hν	Mw_{theo}	Conversion (CTA2)	Conversion (CTA3)
100/1/0/0	395 nm	≈ 10k	Trace	Trace
100/1/0/0	460 nm	≈ 10k	Trace	Trace
100/1/0/0	532 nm	≈ 10k	Trace	Trace
100/1/0.4/0	532 nm	≈ 10k	Trace	Trace
200/1/0.4/3	532 nm	≈ 10k	Trace	Trace

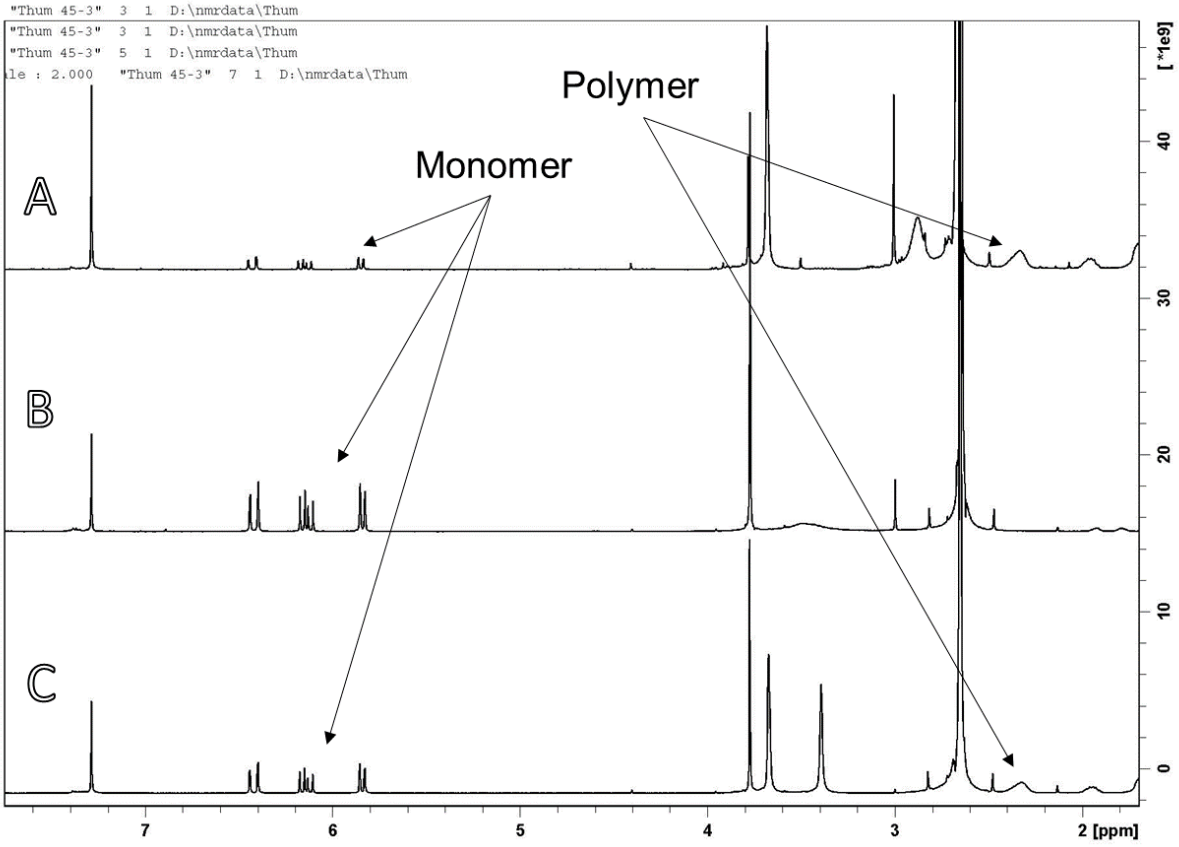

Figure 26. ^{1}H NMR of PET-RAFT polymerization of MA with CTA3 in DMSO after 18 hrs of irradiation at 525 nm. (A) EY and TEA. (B) EY only. (C) no EY.

Without an electron donor, energy transfer from the excited photocatalyst to the CTA is expected to drive C-S bond homolysis. Previous results have shown that direct irradiation of CTA3 does not result in photoRAFT so it is unlikely that C-S bond homolysis can occur from the exited state of CTA3 and thus, energy transfer from EY to CTA3 is not expected to initiate polymerization. PET-RAFT, on the other hand, relies on the reduction of the trithiocarbonate by the photochemically-reduced photocatalyst and has been previously shown to be much more effective than energy transfer.[13] Although there appears to be a higher conversion of monomer when TEA is present, the overall polymer formation is insignificant. One possibility is that electron transfer from reduced eosin y is endergonic, however, electron transfer to structurally similar trithio-based RAFT agents has been previously shown to be energetically favorable.[13] Like in the case of direct irradiation, C-S bond homolysis for the reduced trithiocarbonate is either too short-lived to initiate polymerization, or it is energetically unfavorable leading to rapid back electron transfer and no subsequent polymer formation.

5. Discussion: Computational Analysis

The geometry of cyclic CTAs prepared in this work was investigated using Gaussian 09. The geometry was optimized using B3LPY-6311G. The geometry of the common photoRAFT agent, dibenzyl trithiocarbonate (figure 28), was compared to the cyclic analogue, CTA3, prepared in this study (figure 27). For the common photoRAFT agent dibenzyl trithiocarbonate, the phenyl ring and trithio group are oriented at 90° relative to one another which may enable the stabilization of the transition state during C-S bod homolysis. However, for the structure of CTA3 (Figure 27), the trithio group lies completely out of plain with respect to the rest of the ring. During C-S bond homolysis, the forming phenacyl radical is stabilized by the adjacent phenyl ring, but a sulfur-centered radical must also form on the trithiocarbonate group. When the phenyl ring and trithio groups are oriented at 90°, the electron density at the top and bottom of the aromatic group can stabilize the phenacyl radical and the electron density of the thiocarbonyl group can

be used to stabilize the sulfur-centered radical. In the cyclic analogues such as CTA3, however, the misalignment between the trithio group and the phenyl ring induced by the geometry of the ring does not allow for the forming radical from C-S bond homolysis to be sufficiently stabilized by the thiocarbonyl group. It is likely that the geometry of cyclic trithiocarbonates developed in this work is such that, no polymerization is observed because, in strained systems with an endocyclic trithio carbonate, there is no orbital overlap between the exocyclic phenyl ring and the trithio group in the transition state creating a reaction barrier higher in energy than the excited state of the CTA.

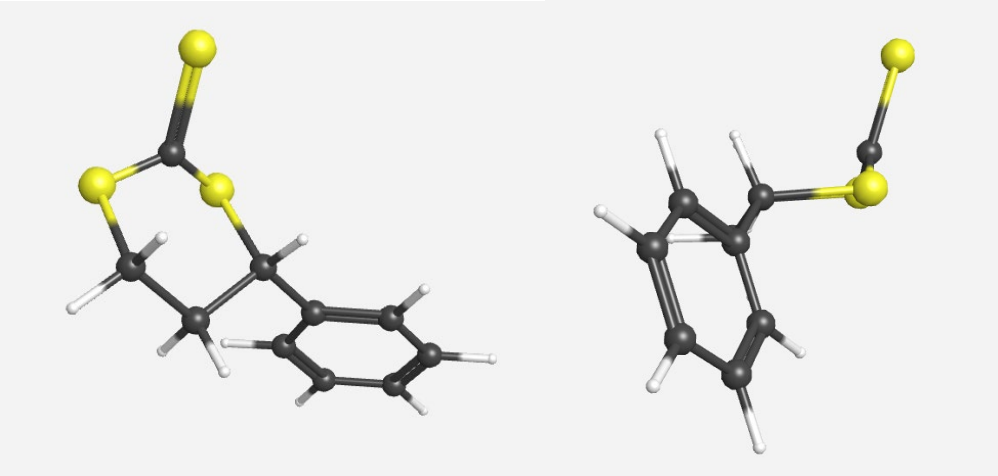

Figure 27. Optimized molecular geometries of the singlet of CTA3 in two different orientations.

Figure 28. Optimized molecular geometries of the singlet of the photoRAFT agent dibenzyl trithiocarbonate in two different orientations.

The geometry of cyclic CTAs with increasing ring size were investigated computationally to determine if an increase in ring size would significantly change the orientation of the phenyl ring with respect to the trithio group. Ring sizes of 7, 8, and 10 were investigated and their optimized geometries are given in figures 29-32. Although, after a 6-membered ring, increasing ring size also increases ring strain, it also increases the number of available conformers which may allow for the relative orientation of the phenyl ring and trithio group to achieve the proper orientation for C-S bond homolysis.

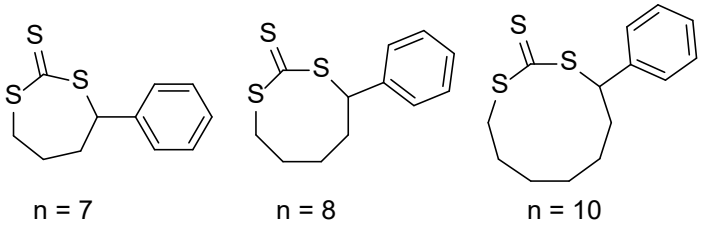

Figure 29. Structures of cyclic CTAs with ring sizes of 7, 8 and 10.

The optimized geometries of cyclic CTAs of n = 7, 8 and 10 are given below in figures 30-32. Despite the increase in ring size, there is no optimized geometry well-suited for C-S bond homolysis. For n = 7, the ring assumes a twist chair-like conformer, but with the thiocarbonyl out of plane with the ring system and the hydrogen atoms adjacent to the phenyl ring in the axial position. For n = 8, the ring assumes a boat-chair type conformer, but with the thiocarbonyl group significantly out of alignment with the adjacent phenyl ring. Cyclodecane, on the other hand, is large enough that it can significantly distort the ring shape to minimize intermolecular interactions. This is evident in the CTA with n = 10 as the thiocarbonyl group is bent back over the ring system and is completely misaligned with respect to the phenyl ring. Despite the increased number of conformers available in larger ring systems, based on the optimized geometries of cyclic CTAs with n = 7, 8 and 10, it is unlikely that they will act as photoiniferters for RAFT polymerization.

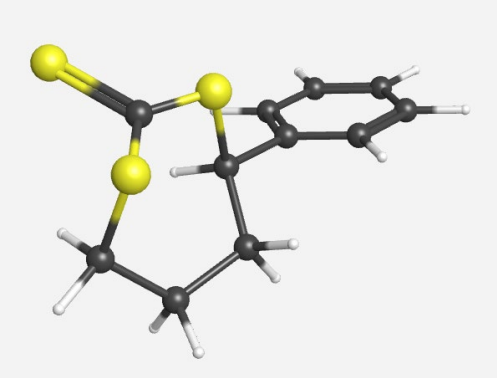

Figure 30. Optimized molecular geometries of n = 7 cyclic CTA.

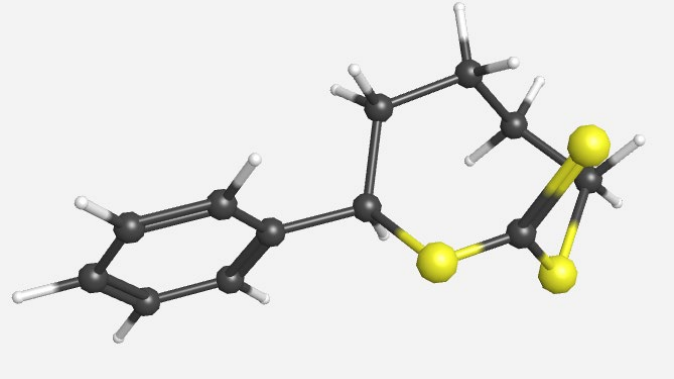

Figure 31. Optimized molecular geometries of n = 8 cyclic CTA.

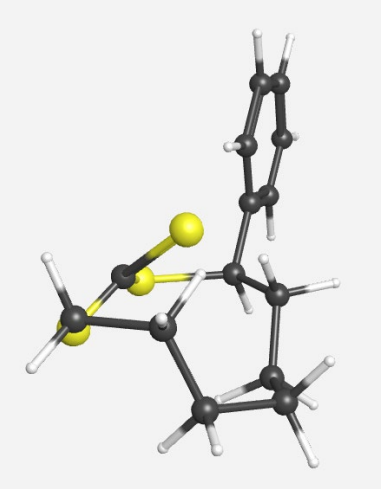

Figure 32. Optimized molecular geometries of n = 10 cyclic CTA.

6. Conclusions.

In this work a new class of cyclic chain transfer agents based on current RAFT agents and TARO-based RAFT agents were synthesized to prepare cyclic polymers using photoRAFT or PET-RAFT. Cyclic CTAs synthesized in this work were evaluated with a series of different monomers, and under various conditions, but no significant polymer formation was observed under any set of experimental conditions. There are two possible explanations for the lack of polymer production under the conditions tested. The first is that C-S bond breakage is endergonic, and the second is that the reactive species formed after bond breakage rapidly react to reform the starting CTA before initiation can occur. Future work could investigate these possibilities by the direct investigation of the intermediates formed after irradiation using transient absorption spectroscopy, but those experiment are outside of the scope of this work. Geometries of the cyclic CTAs were evaluated using computational analysis and the strained ring structure is not ideal for C-S bond homolysis.

7. References.

1. Laurent, B. A.; Grayson, S. M., Synthetic approaches for the preparation of cyclic polymers. *Chem Soc Rev* **2009,** *38* (8), 2202-13.
2. Kricheldorf, H. R., Cyclic polymers: Synthetic strategies and physical properties. *Journal of Polymer Science Part A: Polymer Chemistry* **2010,** *48* (2), 251-284.
3. Haque, F. M.; Grayson, S. M., The synthesis, properties and potential applications of cyclic polymers. *Nature Chemistry* **2020,** *12* (5), 433-444.
4. Xu, X.; Zhou, N.; Zhu, J.; Tu, Y.; Zhang, Z.; Cheng, Z.; Zhu, X., The first example of main-chain cyclic azobenzene polymers. *Macromol Rapid Commun* **2010,** *31* (20), 1791-7.
5. Roovers, J., Viscoelastic Properties of Polybutadiene Rings. *Macromolecules* **1988,** *21* (5), 1517-1521.
6. Chen, R.; Nossarev, G. G.; Hogen-Esch, T. E., Synthesis and thermal and spectroscopic properties of macrocyclic vinyl aromatic polymers. *J Polym Sci Pol Chem* **2004,** *42* (21), 5488-5503.
7. Otsu, T., Iniferter concept and living radical polymerization. *J Polym Sci Pol Chem* **2000,** *38* (12), 2121-2136.
8. You, Y. Z.; Hong, C. Y.; Bai, R. K.; Pan, C. Y.; Wang, J., Photo-initiated living free radical polymerization in the presence of dibenzyl trithiocarbonate. *Macromol Chem Phys* **2002,** *203* (3), 477-483.
9. Lu, L.; Zhang, H. J.; Yang, N. F.; Cai, Y. L., Toward rapid and well-controlled ambient temperature RAFT polymerization under UV-Vis radiation: Effect of radiation wave range. *Macromolecules* **2006,** *39* (11), 3770-3776.

10. Muthukrishnan, S.; Pan, E. H.; Stenzel, M. H.; Barner-Kowollik, C.; Davis, T. P.; Lewis, D.; Barner, L., Ambient temperature RAFT polymerization of acrylic acid initiated with ultraviolet radiation in aqueous solution. *Macromolecules* **2007,** *40* (9), 2978-2980.
11. Ding, C. L.; Fan, C. W.; Jiang, G. Q.; Pan, X. Q.; Zhang, Z. B.; Zhu, J.; Zhu, X. L., Photocatalyst-Free and Blue Light-Induced RAFT Polymerization of Vinyl Acetate at Ambient Temperature. *Macromol Rapid Comm* **2015,** *36* (24), 2181-2185.
12. Pan, X. C.; Tasdelen, M. A.; Laun, J.; Junkers, T.; Yagci, Y.; Matyjaszewski, K., Photomediated controlled radical polymerization. *Progress in Polymer Science* **2016,** *62*, 73-125.
13. Thum, M. D.; Wolf, S.; Falvey, D. E., State-Dependent Photochemical and Photophysical Behavior of Dithiolate Ester and Trithiocarbonate Reversible Addition-Fragmentation Chain Transfer Polymerization Agents. *J Phys Chem A* **2020,** *124* (21), 4211-4222.
14. Bingham, N. M.; Roth, P. J., Degradable vinyl copolymers through thiocarbonyl addition-ring-opening (TARO) polymerization. *Chem Commun (Camb)* **2018,** *55* (1), 55-58.
15. Houillot, L.; Bui, C.; Save, M.; Charleux, B.; Farcet, C.; Moire, C.; Raust, J.-A.; Rodriguez, I., Synthesis of Well-Defined Polyacrylate Particle Dispersions in Organic Medium Using Simultaneous RAFT Polymerization and Self-Assembly of Block Copolymers. A Strong Influence of the Selected Thiocarbonylthio Chain Transfer Agent. *Macromolecules* **2007,** *40* (18), 6500-6509.
16. Sugawara, A.; Sato, T.; Sato, R., Convenient Synthesis of Cyclic Trithiocarbonates from 1,2- or 1,3-Dihaloalkanes and Sodium Trithiocarbonate in the Presence of Phase-Transfer Catalyst. *Bulletin of the Chemical Society of Japan* **1989,** *62* (1), 339-341.
17. Devdutt Chaturvedi Nitin Srivastava, R. K., Novel and Efficient Method for the Synthesis of Cyclic Trithiocarbonates employing Cs2CO3/CS2 system. *Research Journal of Chemistry and Enviornment* **2021,** *25* (12), 142-148.
18. Dong, X. Y.; Zhang, Y. F.; Ma, C. L.; Gu, Q. S.; Wang, F. L.; Li, Z. L.; Jiang, S. P.; Liu, X. Y., A general asymmetric copper-catalysed Sonogashira C(sp(3))-C(sp) coupling. *Nat Chem* **2019,** *11* (12), 1158-1166.
19. Perrier, S., 50th Anniversary Perspective: RAFT Polymerization—A User Guide. *Macromolecules* **2017,** *50* (19), 7433-7447.
20. Chen, M.; Zhong, M.; Johnson, J. A., Light-Controlled Radical Polymerization: Mechanisms, Methods, and Applications. *Chem Rev* **2016,** *116* (17), 10167-211.
21. McKenzie, T. G.; Fu, Q.; Uchiyama, M.; Satoh, K.; Xu, J.; Boyer, C.; Kamigaito, M.; Qiao, G. G., Beyond Traditional RAFT: Alternative Activation of Thiocarbonylthio Compounds for Controlled Polymerization. *Advanced Science* **2016,** *3* (9).
22. Young, J. B.; Bowman, J. I.; Eades, C. B.; Wong, A. J.; Sumerlin, B. S., Photoassisted Radical Depolymerization. *ACS Macro Lett* **2022,** *11* (12), 1390-1395.
23. Hughes, R. W.; Lott, M. E.; Bowman, J. I.; Sumerlin, B. S., Excitation Dependence in Photoiniferter Polymerization. *ACS Macro Lett* **2023,** *12* (1), 14-19.
24. Thum, M. D.; Hong, D.; Zeppuhar, A. N.; Falvey, D. E., Visible-Light Photocatalytic Oxidation of DMSO for RAFT Polymerization. *Photochem Photobiol* **2021,** *97* (6), 1335-1342.
25. Smith, R. A.; Fu, G.; McAteer, O.; Xu, M.; Gutekunst, W. R., Radical Approach to Thioester-Containing Polymers. *J Am Chem Soc* **2019,** *141* (4), 1446-1451.
26. Kiel, G. R.; Lundberg, D. J.; Prince, E.; Husted, K. E. L.; Johnson, A. M.; Lensch, V.; Li, S.; Shieh, P.; Johnson, J. A., Cleavable Comonomers for Chemically Recyclable Polystyrene: A General Approach to Vinyl Polymer Circularity. *J Am Chem Soc* **2022,** *144* (28), 12979-12988.
27. Bingham, N. M.; Nisa, Q. u.; Chua, S. H. L.; Fontugne, L.; Spick, M. P.; Roth, P. J., Thioester-Functional Polyacrylamides: Rapid Selective Backbone Degradation Triggers Solubility Switch Based on Aqueous Lower Critical Solution Temperature/Upper Critical Solution Temperature. *ACS Applied Polymer Materials* **2020,** *2* (8), 3440-3449.
28. Meijs, G. F.; Rizzardo, E.; Le, T. P. T.; Chen, Y.-C., Influence of thionoesters on the degree of polymerization of styrene, methyl acrylate, methyl methacrylate and vinyl acetate. *Die Makromolekulare Chemie* **1992,** *193* (2), 369-378.

29. Xu, J.; Shanmugam, S.; Duong, H. T.; Boyer, C., Organo-photocatalysts for photoinduced electron transfer-reversible addition–fragmentation chain transfer (PET-RAFT) polymerization. *Polymer Chemistry* **2015,** *6* (31), 5615-5624.
30. Figg, C. A.; Hickman, J. D.; Scheutz, G. M.; Shanmugam, S.; Carmean, R. N.; Tucker, B. S.; Boyer, C.; Sumerlin, B. S., Color-Coding Visible Light Polymerizations To Elucidate the Activation of Trithiocarbonates Using Eosin Y. *Macromolecules* **2018,** *51* (4), 1370-1376.